Bled Workshops
in Physics
Vol. 19, No. 2

Proceedings to the 21*st Workshop*
What Comes Beyond . . . *(p. 261)*
Bled, Slovenia, June 23–July 1, 2018

12 On Triple-periodic Electrical Charge Distribution as a Model of Physical Vacuum and Fundamental Particles

E.G. Dmitrieff *

Irkutsk State University, Russia

Abstract. In this study we consider triple-periodical electrical charge distributions with the pattern similar to the Weaire-Phelan structure. According to it, the space is splitted to opposite-charged cells separated with electrically neutral border.

Possible configurations obtained as results of exchanges of these cells appear to have properties that can be corresponded to the quantum numbers of known fundamental particles.

We find it promising to use models of this kind, aiming to infer the axioms and constants of the Standard Model from the emergent geometrical properties of the distribution.

Povzetek. Prispevek obravnava trojne periodične porazdelitve električnih nabojev, ki imajo vzorec podoben Weaire-Phelan strukturam. V modelu je prostor razdeljen na celice z nasprotnimi naboji, ki jih loči električno nevtralna meja.

Konfiguracije, ki sledijo z izmenjavo teh celic, imajo lastnosti, ki jih avtor poveže s kvantnimi števili kvarkov in leptonov.

Avtor meni, da ti modeli omogočijo izpeljavo privzetkov in konstant standardnega modela.

Keywords: Particle model,Weaire-Phelan tessellation

12.1 Introduction

The spin-charge-family theory presented in [1], [2], [8], [9] offers reasonable explanations for the phenomena of the Standard Model of the fundamental particles. Originating from Clifford algebra, it comes to the binary internal degrees of freedom, explaining properties of existing fundamental particles and predicting existence of extra fermion families.

In turn, we reproduce particle properties starting with *binary code* model. As we have shown in [7], Boolean models designed for fundamental particles can reproduce most of their properties, including charges (electrical, color, weak and hyper-charge), lepton- and baryon numbers, fermion flavor and family membership, and boson spin magnitude. The particles are represented as combinations or *codes* of symbols carrying one of two possible values, so these models are *binary*.

* E-mail: eliadmitrieff@gmail.com

Developing these models, we started with well-known linear codes, that consist of binary digits (*bits*) with usual values either 1 or 0. Then, in order to reduce the amount of information carried by the code, we abandoned the linear structure in favor of spatial one. Also we have symmetrized and normalized the values carried by bits, using $+\frac{1}{6}$ and $-\frac{1}{6}$ instead of 1 and 0. These values could be directly interpreted as electrical charge in units of electron charge e.

Using spatial combination of eight symbols of this kind, we managed to represent all known fundamental particles. Also, analyzing unused combinations, we proposed existence of new scalar particle forming the vacuum condensate. It could be represented by this combination that is repeated periodically, filling the space as a tessellation.

Since the tessellation can be chiral, the space filled with small alternating charged regions, comparing to simple empty space, has an advantage of offering possible explanation for difference between right- and left-handed particles in respect of the vacuum.

Different particle codes, substituting vacuum codes in the tessellation, violate the periodicity with different ways. We suppose that it may be used to infer associated rest energies (masses) instead of postulating them.

Treating vacuum expectation value as Coulomb potential between neighboring opposite-charged "bits" [11], we estimated that the distance between them should be on scale of $\approx 10^{-21}$m.

Being inspired by idea of vacuum domains [3], we suppose that the interpretation of these "bits" as domains can explain the problem of their observations absence. As asserted originally by Zeldovich with co-authors, the vacuum domains should appear as consequence of symmetry break in the phase transition. In our models, they do exist but have the correlation radius on sub-particle scale instead of cosmological one. This should happen in case the 2-order phase transition is not yet complete but just approaches its critical point.

Having a model with some spatial distribution of charged bits, or vacuum domains, we recognize that it is necessary to find out the pattern of this distribution which is consistent with other observable properties of vacuum and particles, including their symmetry, mass spectrum, propagation, interactions and so on.

After checking simple (**NaCl**-like) and volume-centered (**CsCl**-like) cubic lattices, we found out that the A15 ($\mathbf{Nb_3Sn}$-like) lattice, or Weaire-Phelan structure, has some advantages allowing it to be the possible vacuum- and particle model.

12.2 Overview of the original Weaire-Phelan tessellation

The original Weaire-Phelan structure is described in [12]. It is a foam of equal-volumed cells separated by thin walls. Among other structures, having the same cell volume, this one has the minimal (known at the present time) inter-cell wall area, so it is a candidate solution for the Kelvin problem [14]. There is evidence of self-assembling of this tessellation driven by minimization of the surface energy [13].

Cells forming the Weaire-Phelan structure have almost flat faces and just slightly curved edges, thus they can be closely approximated by irregular polyhe-

dra. It is nesessary to use two *kinds* of them – dodecahedra (D) and tetrakaidecahedra (T)[1].

Unlike dodecahedra, the tetrakaidecahedra have three possible *orientations* in respect of the three Cartesian axes.

The cells of both kinds can be included in the tessellation in two ways, so they became *chiral*.

Eight cells, differing in kind, chirality, and orientation, form one translation unit. These translation units, in turn, form simple cubic grid.

Assuming the size of translation unit to be $l = 4\lambda$ in each dimension (where λ is a scale factor, and 4 is used to get most of coordinates integer), we get the unit volume $V_u = l^3 = 64\lambda^3$, and cell volume $V_c = \frac{1}{8}V_u = 8\lambda^3$ (remembering that all cells are equal-volumed).

Having the coordinate axes perpendicular to the hexagonal faces of the tetrakaidecahedra, and associating the origin with the center of one of dodecahedra, one can obtain coordinates of the centers of all other cells:

	D	T_x	T_y	T_z
R	(0,0,0)	(0,2,1)	(1,0,2)	(2,1,0)
L	(2,2,2)	(0,2,3)	(3,0,2)	(2,3,0)

These coordinates are expressed in units of λ and derermined up to 4λ, meaning that one can obtain coordinates of each cell by adding of "even" vector

$$\mathbf{V}_E = (4n_x, 4n_y, 4n_z)\,\lambda, n_i \in \mathbb{Z}. \tag{12.1}$$

Further, we omit the scale factor λ where it shouldn't cause misunderstanding.

Here we chose the R and L mark of the chirality by the arbitrary choice.

There are four symmetry axis C_3 defined by equations $\pm x = \pm y = \pm z$.

Since the structure does not possess reflection symmetry, it is chiral, so there are two mirror-reflected structures. For instance, after reflecting in the plane $x = y$ the chirality is reversed and the coordinates are changed as the following:

	D	T_x	T_y	T_z
L	(0,0,0)	(2,0,1)	(0,1,2)	(1,2,0)
R	(2,2,2)	(2,0,3)	(0,3,2)	(3,2,0)

After performing the shift (move) of the whole infinite structure with the "odd" vector

$$\mathbf{V}_O = \mathbf{V}_E + (\pm 2, \pm 2, \pm 2)\lambda, \tag{12.2}$$

[1] The dodecahedron is a pyrithohedron with twelve equal pentagonal faces, possessing terrahedral symmetry T_h, and the tetrakaidecahedron is truncated hexagonal trapezohedron posessing rotoreflextion symmetry C_{3h}, with two hexagonal faces, four large and eight small pentagonal faces.

i.e. for the half-size of the translation unit ($2\sqrt{3}\lambda$), in direction of C_3 axis, we get the original structure again:

	D	T_x	T_y	T_z
L	(2,2,2)	(2,0,3)	(2,3,0)	(1,2,0)
R	(0,0,0)	(0,2,1)	(2,1,0)	(1,0,2)

Thus, the structure possesses global **PS** symmetry, where **P** is parity (particularly, exchange of any two coordinates) and **S** is shift along C_3 axis on the half of translation unit size (or, generally, on the odd vector).

It also means that despite of mirror asymmetry of each finite part, there is only one infinite Weaire-Phelan structure, which is either right- or left-handed depending on the choice of origin. It can be also considered as *two* overlapped chiral structures consisting of the same elements but shifted in respect of each other with the odd vector (12.2).

12.3 Dual-charged Weaire-Phelan structure

To use the Weaire-Phelan structure as a spatial version of binary-code model, we need to assume that each cell carries electrical charge with magnitude of $\frac{1}{6}$. Since the space containing no particles is electrically neutral, the counts of positive and negative cells in any volume $\gtrsim l^3$ should be the same. Any change of cell charge, that can be from $+\frac{1}{6}$ to $-\frac{1}{6}$, or back, would cause the total electric charge to change on $\pm\frac{1}{3}$. Thus, all the particles in this model will have discrete charges with step of $\frac{1}{3}$, that is according to experiments. So the existence of particles with charges, for instance, of $\pm\frac{1}{2}$, is impossible.

In general, the charge *inside* cells can be distributed being determined by physical law acting on this scale, for instance:

- all the charge can be concentrated in cell centers, in point-size sub-particles (partons or rishons);
- the charge can be distributed smoothly inside cells around their centers, falling to zero on the inter-cell borders;
- the charges of opposite sign can be concentrated on both sides of the walls between opposite-charged cells, and also can be smoothly distributed along them.

In the following subsections we consider these simplified assumptions of the charge distribution.

We assume that the basic "vacuum" alteration of charged cells in the tessellation should fulfill the following requirements:

- each translation unit should be electrically neutral, and
- cells with opposite chirality should also be opposite-charged.

So, we assume positive charge of cells of one chirality and negative for another. However, at this stage we do not recognize any natural rule that would define the absolute chirality. So, there are $2^3 = 8$ choices of T_i charges and also 2 choices of D. We make this choice as shown in the following table:

Cell type	Charge	Coordinates	Plane
D_R	$-$	$(0,0,0)$	$x+y+z=4n$
T_{Ri}	$+$	$(0,2,1),(1,0,2),(2,1,0)$	$x+y+z=4n+3$
D_L	$+$	$(2,2,2)$	$x+y+z=4n+2$
T_{Li}	$-$	$(0,2,3),(3,0,2),(2,3,0)$	$x+y+z=4n+1$

In the last column of the table we show the equations of planes that contain all the cell centers of particular type.

Making the choice of charge sign for T_i, we break the symmetry between C_3 axis, so one of them becomes dedicated. Also, making this choice for D cell charge breaks symmetry between opposite handednesses. So there are two possible dual-charged Weaire-Phelan structures. That corresponds to the principal possibility of physical vacuum with reversed chirality.

12.4 Cell Centers approximation

Here we abstract from the details of spatial distribution of the electric charge, and suppose it is just concentrated somewhere in the vicinity of the cell centers. We do so to simplify the charge calculation, replacing the integration of the charge density in the volume of interest with counting the number of centers of positive and negative cells falling into it. Since the coordinates of the cell centers are integers (i.e., proportional to the scale factor λ), they can lay on the certain planes only, between which, in this approximation, there is nothing.

12.4.1 CPS symmetry

The following set of grids (Fig. 12.1) illustrates the placement of positive and negative cells' centers, as black and white circles, respectively, in the cubic translation unit of size $4 \times 4 \times 4$ starting with its left bottom front corner from the origin of reference frame. Centers of D-cells are marked with double-border.

The first grid is the cross-section for plane $z = 0$, the second one is for plane $z = 1$ and so on. The plane $z = 4$ is the same as $z = 0$ due to the periodicity.

Considering the translation unit cube that is shifted with the "even" vector $(2n+1)(2,2,2)$, for instance $(-2,-2,-2)$, i.e. performing **S** operation, we get the scheme on the Fig. 12.2 (the first grid is plane $z = -2$ and so on).

After reflecting in the plane $x = y$ (**P** operation) we get the scheme on the Fig. 12.3.

One can ensure that this shift operation (**S**) followed by reflection (**P**) has the same result as the charge inversion (**C**). So these three operations being applied

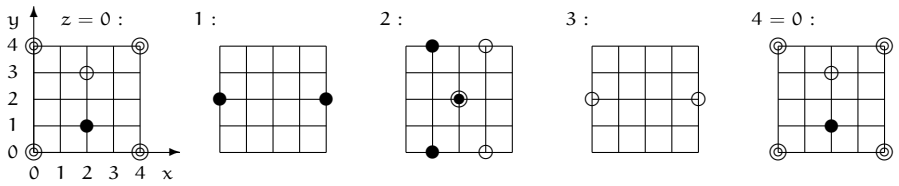

Fig. 12.1. The placement positive- and negative-charged cell centers in the translation unit

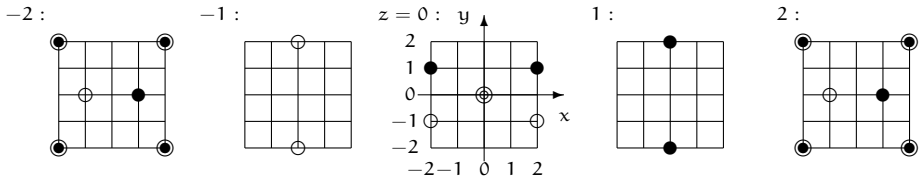

Fig. 12.2. The translation unit after **S** (shift) operation

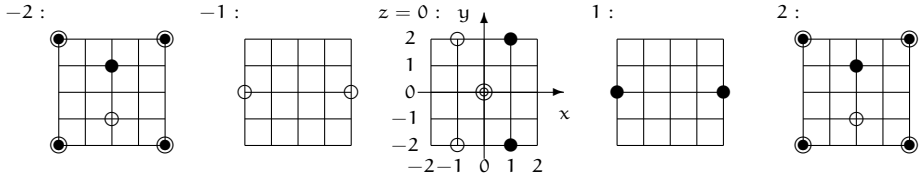

Fig. 12.3. The translation unit after sequential shift and reflection **SP**

consequently (in any order) turn the structure back to its original state. It means that the structure possesses the symmetry in respect of **CPS** combination, but neither in respect of **C**, **P**, **S** individually nor in respect of their pairs **CP**=**PC**=**S**, **PS**=**SP**=**C**, **CS**=**SC**=**P**.

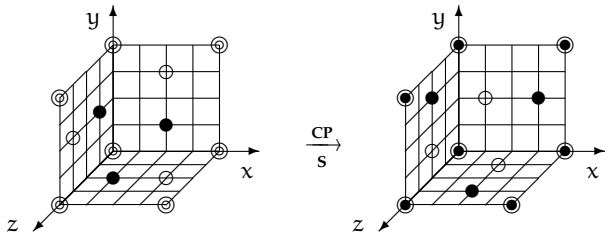

Fig. 12.4. Either **CP** or **S** operation applied to the translation unit

12.4.2 View in isometric projection

The distribution of charged cell centers also can be represented in the reference frame $\xi\zeta\upsilon$, in which ζ axis follows the diagonal of the translation unit cube. The planes containing cells of one type, that are $x + y + z = 4n + k = \zeta$, are planes $\xi\upsilon$.

We perform the reference frame transformation $xyz \mapsto \xi\zeta\upsilon$ using $O(3)$ rotation matrix with Euler angles $\frac{\pi}{4}$ and $\arccos\sqrt{\frac{2}{3}}$:

$$\begin{pmatrix}\xi\\ \zeta\\ \upsilon\end{pmatrix} = \frac{1}{\sqrt{6}}\begin{pmatrix}\sqrt{3} & 0 & -\sqrt{3}\\ \sqrt{2} & \sqrt{2} & \sqrt{2}\\ -1 & 2 & -1\end{pmatrix}\begin{pmatrix}x\\ y\\ z\end{pmatrix}. \tag{12.3}$$

The diagram on Fig. 12.5 illustrates six faces of the translation unit with the center in the point $(0,0,0)$ (the cell center in this point is not shown since it does not belong to the cube's faces). The plane $\xi\upsilon$ is faced to the observer while the ζ axis directs away from the observer.

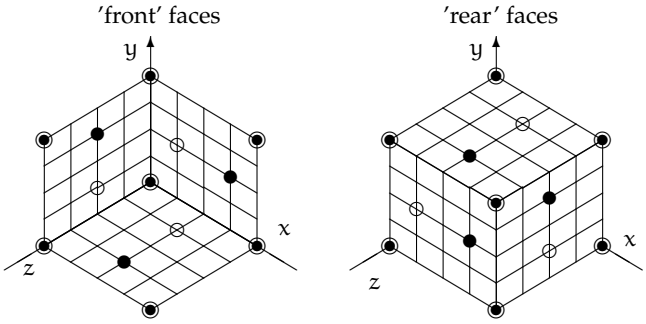

Fig. 12.5. Translation unit cube with the center in $(0,0,0)$ in the isometric projection on its diagonal

The projection to the $\zeta\upsilon$ plane (Fig. 12.6) illustrates that in each translation unit cube there are 12 planes perpendicular to its diagonal (ζ axis), that contain charged cell centers, and that these planes are different. Starting from the 0^{th} plane with $\zeta = 0$, and increasing ζ by $\frac{1}{\sqrt{3}}$, one can found that it is just the 12^{th} one at $\zeta = 12/\sqrt{3}$, where the next translation unit starts, is the same with the 0^{th} plane).

However, planes starting from the translation unit center (the 6^{th}, $\zeta = 6/\sqrt{3}$) repeat planes from 0^{th} through 5^{th} but reversed in charge. Since the translation in ζ direction on $6/\sqrt{3}$ is the **S** operation, that is equal to **CP**, they are also mirrored, i.e. parity-inversed.

So any change in this structure, that is possible in any particular place, can have its "anti-change", with opposite charge and parity, possible in places shifted on some "odd" vector $\mathbf{V}_O$ (12.2).

The diagram on Fig. 12.7 illustrates the placement of the cell centers in the projection on the $\upsilon\xi$ plane:

On this diagram the cells residing on the same plane perpendicular to the ζ axis are joined together with lines and labeled with values of ζ coordinate (in units of $1/\sqrt{3}$), so one can see the *equilateral triangles* that they form[2].

[2] The visible 'constellations' of T cell centers do not form equilateral triangles in the $\upsilon\xi$ planes since they have different ζ.

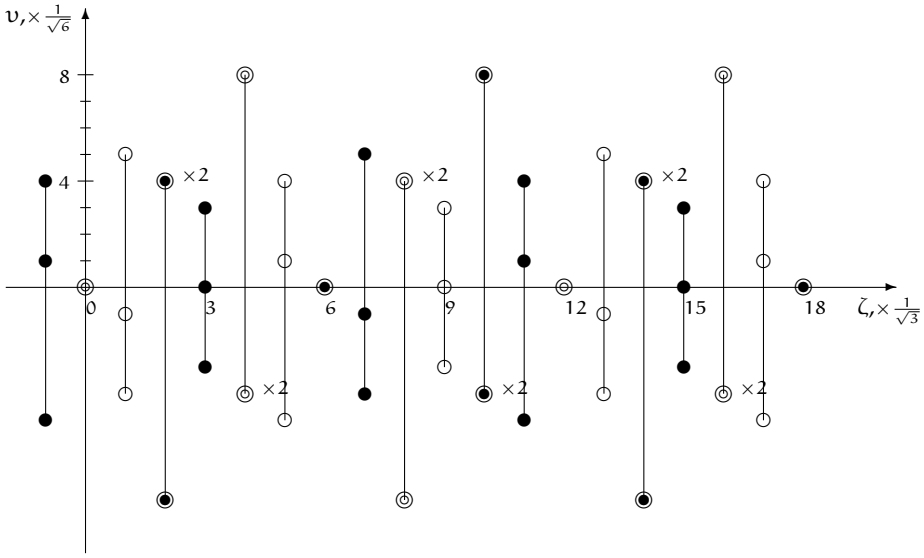

Fig. 12.6. Charged cell centers distribution in projection to the ζυ plane

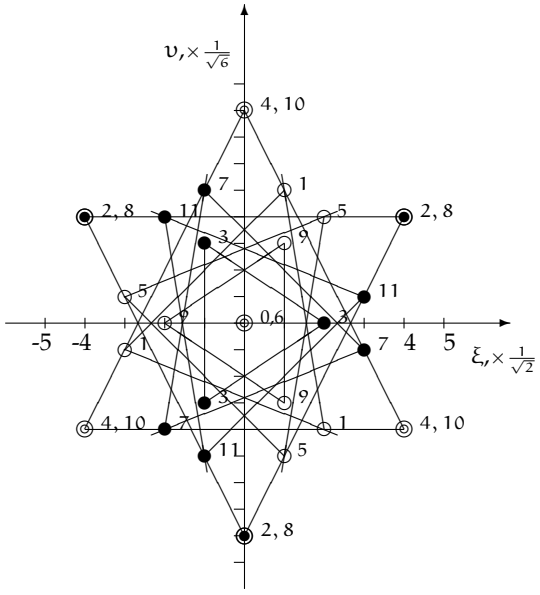

Fig. 12.7. Cell centers placement in projection on the υξ plane

The D cells of different charge overlap and hide each other along the projective direction, so behind each positive cell the negative one is assumed, and vice versa.

The planes, cell types and the shapes the cell centers form, are listed in the Table 12.1, from $\zeta = 0$ to $12/\sqrt{3}$.

$\zeta, \times \frac{1}{\sqrt{3}}$	kind, charge	shape	size	shape description
0	D−	◎	−	Axial D−
1	T−	○ ○ ○	$\sqrt{14}$	Large T− triangle counterclockwise
2	D+	◉ ◉ ◉	$\sqrt{32}$	D+ triangle υ-down
3	T+	● ● ●	$\sqrt{6}$	Small T+triangle (ξ-right)
4	D−	◎ ◎ ◎	$\sqrt{32}$	D− triangle υ-up
5	T−	○ ○ ○	$\sqrt{14}$	Large T− triangle clockwise
6	D+	◉	−	Axial D+
7	T+	● ● ●	$\sqrt{14}$	Large T+ triangle clockwise
8	D−	◎ ◎ ◎	$\sqrt{32}$	D− triangle υ-down
9	T−	○ ○ ○	$\sqrt{6}$	Small T− triangle (ξ-left)
10	D+	◉ ◉ ◉	$\sqrt{32}$	D+ triangle υ-up
11	T+	● ● ●	$\sqrt{14}$	Large T+ triangle counterclockwise
12	D−	◎	−	Axial D−

Table 12.1. Shapes of cell center placements in twelve different planes

12.4.3 Small T triangle and its environment

Consider the small triangle of three T+ cells with the same charge at $\zeta = 3/\sqrt{3}$, with edge of $\sqrt{6}$. The triangle has electric charge $\Sigma q_3 = +1/2$, so its environment has the opposite charge $q_{env} = -1/2$ that ensures the total electrical neutrality.

The closest neighborhood of the small T triangle is asymmetrical: in ζ direction, there are two planes with *different* charge before it and two *negative*-charged planes after it.

Namely, at $\zeta = 1/\sqrt{3}$ there is a large (edge is $\sqrt{14}$) T− triangle carrying electric charge $q = -1/2$, and at $\zeta = 2/\sqrt{3}$ there is a D+ triangle (edge=$\sqrt{32}$) carrying $q = +1/2$, altogether $q = 0$.

On the contrary, at the two following planes ($\zeta = 4/\sqrt{3}$ and $\zeta = 5/\sqrt{3}$) there are triangles with the same structure as before, but *both* are negative-charged, carrying together $q = -1$.

The same structure, due to the **CPS** symmetry, exists around small T− triangle at $\zeta = 9/\sqrt{3}$, with all the charges (and parity) inverted: both of the triangle in this position, and of its environment.

12.4.4 Choosing the translation unit cell

In our approach, the translation unit is a substitution for concept of a point of space, as a place where a particle can reside.

Instead, a particle in the point is represented as some anti-structural defects located in the corresponding translation unit, so the presupposed concepts of a particle or material point gets unnecessary.

Since the translation unit of dual-charged Wheaire-Phelan structure consists of eight different binary elements (i.e. cells charged $\pm\frac{1}{6}e$), the translation unit has eight internal binary degrees of freedom pretending to replace the curled up dimensions in Kaluza-Klein theories [4], [5], [6], [1], [2], [8], [9].

The translation unit cell can be chosen arbitrary as long as it includes eight structure cells of different geometry[3] [10].

The primitive translation unit cell is a body-centered cube (Fig. 12.5). Most of cells included in it are cross-sectioned by the imaginary borders of the unit cell. It is not quite useful for modeling purposes. Namely, the T cells are taken by halves and while one D cell is taken by eighth parts, another one, residing in the cube's center, is included as whole.

Intending to study defects in the periodical structure, we choose the non-primitive unit so the cells that would participate in the exchange are included as whole, without cross-section.

We found also possible to include additional cells, that would overlay cells with the same geometry while translating, in case these add-ons appear as mutually compensating pairs of cells having opposite parity and also opposite electrical charge.

So we choose the neutral translation unit that consist of 3 positive charged cells of small T-triangle at $\zeta = 3/\sqrt{3}$, that would participate in the exchange, and *halves* of negative charged cells of two large T-triangles both at $1/\sqrt{3}$ and at $5/\sqrt{3}$, that would remain unchanged.

We do not consider the changes that may occur in cells of *large* T triangles since each T cell belonging to any *small* triangle in one chiral sub-lattice also belongs to a large triangle in another, mirror-reflected sub-lattice.

12.4.5 Anti-structure defects

Now we consider the *inversion* of the electric charge that can occur in particular cell or cells for some reason. Namely, it should happen as result of an interaction. Since the electric charge is conserved, the inversion in any particular cell must be accompanied by reverse inversion in another cell nearby, so all the inversions are, in fact, te results of *exchanges*.

However, we focus on possible single, double and triple inversions in the cells of small T triangle supposing that the corresponding reverse inversions are migrated or propagated into some location that is enough far away.

[3] See the above in this section 12.2.

Also, we can examine just one small T triangle of two, for instance, at $\zeta = 3/\sqrt{3}$; another small T triangle at $\zeta = 9/\sqrt{3}$ is located in position shifted on half-unit size, so the latter should have the same properties as the first one, but **CP**-ed, i.e. charge-inverted and mirror-reflected.

Consider the small T+triangle accompanied by several cells in its closest neighborhood, keeping total electrical charge of them to be zero (Σq_n means the electric charge of three cell with the center at n-th plane, i.e. with $\zeta = n/\sqrt{3}$):

$$\begin{aligned}
Q &= \Sigma q_1 + \Sigma q_3 = -\frac{1}{2} + \frac{1}{2} = 0, \text{ or} \\
Q &= \Sigma q_3 + \Sigma q_5 = \frac{1}{2} - \frac{1}{2} = 0, \text{ or} \\
Q &= \frac{\Sigma q_1 + \Sigma q_5}{2} + \Sigma q_3 = 0, \text{ or} \\
Q &= q_0 + \frac{\Sigma q_1}{2} + \Sigma q_3 + \frac{\Sigma q_5}{2} + q_6 = 0, \text{ or} \\
Q &= q_0 + \Sigma q_1 + \Sigma q_3 + q_6 = -\frac{1}{6} - \frac{1}{2} + \frac{1}{2} + \frac{1}{6} = 0, \text{ or} \\
Q &= q_0 + \frac{\Sigma q_1}{2} + \frac{\Sigma q_2}{2} + \Sigma q_3 + \frac{\Sigma q_4}{2} + \frac{\Sigma q_5}{2} + q_6 = 0.
\end{aligned} \tag{12.4}$$

In all the cases, $Q = \Sigma q_3 + q_{env} = 0$, while $\Sigma q_3 = +\frac{1}{2}$, so the environment charge $q_{env} = -\frac{1}{2}$.

It is obvious that this q_{env} is determined by T-cells only, since it is a charge of initially neutral vacuum after "removing" three positive-charged T+cells forming the small triangle and keeping the original count of D cells. So there are three extra negative-charged T-cells while all the D-cells still compensate each other:

$$\begin{aligned}
q_{env} = & q^T_{env} = -\frac{1}{2}; \\
& q^D_{env} = 0.
\end{aligned} \tag{12.5}$$

Each plane of T-cells *before* the small triangle in ζ-oder has its corresponding equal-charged plane *after* it at the same distance (for instance, at $\zeta = 1/\sqrt{3}$ and $5/\sqrt{3}$). This symmetry requires a half of environment charge, that is determined by T sub-lattice, to be resided before the small triangle plane $\zeta = 3/\sqrt{3}$, and another half to be resided after it:

$$\begin{aligned}
q^T_{env}(\zeta < \frac{3}{\sqrt{3}}) &= -\frac{1}{4}; \\
q^T_{env}(\zeta > \frac{3}{\sqrt{3}}) &= -\frac{1}{4}.
\end{aligned} \tag{12.6}$$

Due to the **CPS** symmetry, we also have

$$\begin{aligned}
q^T_{env}(\zeta < \frac{9}{\sqrt{3}}) &= +\frac{1}{4}; \\
q^T_{env}(\zeta > \frac{9}{\sqrt{3}}) &= +\frac{1}{4}
\end{aligned} \tag{12.7}$$

for the environment of the negative-charged small T-triangle at $\zeta = 9/\sqrt{3}$.

12.4.6 Handedness change as Exchange of D triangles

Although D-sublattice has no influence on the total charge of the small T+triangle's environment q_{env} (12.5), exchanges in it can redistribute the electric charge between *rear* ($\zeta < \frac{3}{\sqrt{3}}$) and *front* ($\zeta > \frac{3}{\sqrt{3}}$) half-spaces because it is asymmetric in respect of the plane ($\zeta = 3/\sqrt{3}$).

We examine such exchanges whether they can be used to represent the particle's handedness that also does not influence on its charge.

Following the model that assumes the charge is located closely to the cell centers, we must conclude that D triangles just before and after small triangle at $\zeta = 3/\sqrt{3}$ have the charges

$$\begin{aligned} \Sigma q_2 &= q^D(\zeta = \frac{2}{\sqrt{3}}) = +\frac{1}{2}, \\ \Sigma q_4 &= q^D(\zeta = \frac{4}{\sqrt{3}}) = -\frac{1}{2}, \end{aligned} \tag{12.8}$$

and in case they exchange, the charge of 1 will redistribute from rear half-space to the front one[4].

However, considering the case when the charge of cells is *not* concentrated in their centers, being instead distributed on radii comparable to the inter-centers distance ($\approx 2 \ldots \sqrt{5} \approx 2.236$), we recognize that the charge of cells in plane $\zeta = 2/\sqrt{3}$ would not reside just *before* the plane $\zeta = 3/\sqrt{3}$. It is so because the offset between these planes is significantly less than the inter-center distance: $1/\sqrt{3} \approx 0.577 < 2$ (Fig. 12.8), and is comparable with the distribution radius. That is why one should assert that some part of q_2 would reside *after* the plane $\zeta = 3/\sqrt{3}$, and some part of q_4 would, in turn, reside *before* it (see Fig. 12.8).

To be the representation of the reversed handedness, the D-exchange operation should redistribute only the half of the charge (12.8). This requirement is fulfilled in case a quarter of the charge of each D-cell in triangles is distributed on the other side of the plane $\zeta = 3/\sqrt{3}$ that is located at the $1/\sqrt{3}$ of its center. So we can use this condition to obtain more realistic rule of the charge distribution rather than simple charged point in the cell center. Now we use the *halved* values of (12.8), that are equal to q^T_{env} by the magnitude, so they can effectively compensate them:

$$\begin{aligned} q^{D*}(\zeta = \frac{2}{\sqrt{3}}) &= +\frac{1}{4}, \\ q^{D*}(\zeta = \frac{4}{\sqrt{3}}) &= -\frac{1}{4}, \end{aligned} \tag{12.9}$$

In this case,

$$\begin{aligned} q_{env}(\zeta < \frac{3}{\sqrt{3}}) &= q^T_{env}(\zeta < \frac{3}{\sqrt{3}}) + q^{D*}(\zeta = \frac{2}{\sqrt{3}}) = -\frac{1}{4} + \frac{1}{4} = 0; \\ q_{env}(\zeta > \frac{3}{\sqrt{3}}) &= q^T_{env}(\zeta > \frac{3}{\sqrt{3}}) + q^{D*}(\zeta = \frac{4}{\sqrt{3}}) = -\frac{1}{4} - \frac{1}{4} = -\frac{1}{2}, \end{aligned} \tag{12.10}$$

[4] Such an exchange also can be considered as a rotation of a spatial hexagon containing all six cell centers of the both D-triangles, with the angle of 60° in any direction

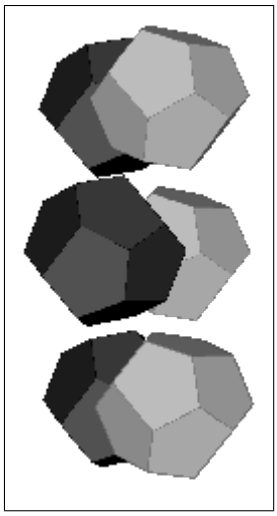

Fig. 12.8. Visually overlapping cells of two D triangles with $\zeta = 2/\sqrt{3}$ and $\zeta = 4/\sqrt{3}$ in polyhedral approximation

and after exchange between D-triangles at $\zeta = 2/\sqrt{3}$ and $4/\sqrt{3}$ they would turn into

$$\begin{aligned} q_{env}(\zeta < \frac{3}{\sqrt{3}}) &= q^{T}_{env}(\zeta < \frac{3}{\sqrt{3}}) + q^{D*}(\zeta = \frac{2}{\sqrt{3}}) = -\frac{1}{4} - \frac{1}{4} = -\frac{1}{2}; \\ q_{env}(\zeta > \frac{3}{\sqrt{3}}) &= q^{T}_{env}(\zeta > \frac{3}{\sqrt{3}}) + q^{D*}(\zeta = \frac{4}{\sqrt{3}}) = -\frac{1}{4} + \frac{1}{4} = 0. \end{aligned} \tag{12.11}$$

So we can use them to represent weak isospin and weak hypercharge for "down" particles:

$$T_3^{down} = q_{env}(\zeta < \frac{3}{\sqrt{3}}) = \frac{1}{2}(\Sigma q_1 + \Sigma q_2) \tag{12.12}$$

$$Y_W^{down}/2 = \Sigma q_3 + q_{env}(\zeta > \frac{3}{\sqrt{3}}) = \Sigma q_3 + \frac{1}{2}(\Sigma q_4 + \Sigma q_5) \tag{12.13}$$

At $\zeta = 9/\sqrt{3}$, the small T-triangle and its neighborhood are inverted in respect to $\zeta = 3/\sqrt{3}$ due to the **CPS** symmetry, so original

$$\begin{aligned} q_{env}(\zeta < \frac{9}{\sqrt{3}}) &= q^{T}_{env}(\zeta < \frac{9}{\sqrt{3}}) + q^{D*}(\zeta = \frac{8}{\sqrt{3}}) = +\frac{1}{4} - \frac{1}{4} = 0; \\ q_{env}(\zeta > \frac{9}{\sqrt{3}}) &= q^{T}_{env}(\zeta > \frac{9}{\sqrt{3}}) + q^{D*}(\zeta = \frac{10}{\sqrt{3}}) = +\frac{1}{4} + \frac{1}{4} = +\frac{1}{2} \end{aligned} \tag{12.14}$$

would turn after D-exchange into

$$\begin{aligned} q_{env}(\zeta < \frac{9}{\sqrt{3}}) &= q^{T}_{env}(\zeta < \frac{9}{\sqrt{3}}) + q^{D*}(\zeta = \frac{8}{\sqrt{3}}) = +\frac{1}{4} + \frac{1}{4} = +\frac{1}{2}; \\ q_{env}(\zeta > \frac{9}{\sqrt{3}}) &= q^{T}_{env}(\zeta > \frac{9}{\sqrt{3}}) + q^{D*}(\zeta = \frac{10}{\sqrt{3}}) = +\frac{1}{4} - \frac{1}{4} = 0, \end{aligned} \tag{12.15}$$

and both the values $q_{env}(\zeta < \frac{9}{\sqrt{3}})$ and $\Sigma q_9 + q_{env}(\zeta > \frac{9}{\sqrt{3}})$ would, again, coincide with weak isospin T_3 and weak hypercharge $Y_W/2$ for "up" fermions, respectively:

$$T_3^{up} = q_{env}(\zeta < \frac{9}{\sqrt{3}}) = \frac{1}{2}(\Sigma q_7 + \Sigma q_8) \tag{12.16}$$

$$Y_W^{up}/2 = \Sigma q_9 + q_{env}(\zeta > \frac{9}{\sqrt{3}}) = \Sigma q_9 + \frac{1}{2}(\Sigma q_{10} + \Sigma q_{11}) \tag{12.17}$$

So the exchange between D triangles (or, that is the same, rotation of the distorted D hexagon) can be used as a model representing switching between two handednesses.

12.4.7 Down fermions as Inversions in small T+triangle

Inverting charges of cells it the small T+triangle q_3, namely of $q(2,1,0)$, $q(2,1,0)$ and $q(2,1,0)$ in (x,y,z) reference frame[5], one can get eight possible cases (Table 12.2). The total electric charge Q, that changes with steps of $\pm\frac{1}{3}$ according to the count of inverted cells, coincides with the electric charge of eight "down"[6] fermions.

$T_3 :=$ $q_{(<3)}$	q_3^{210}	q_3^{102}	q_3^{021}	Σq_3	$q_{(>3)}$	$\frac{Y_W}{2} :=$ $q_{(\geq 3)}$	Q	symbol
	+	+	+	+1/2		0	0	$\tilde{\nu}_L$
	−	+	+					d_R^{c1}
	+	−	+	+1/6		−1/3	−1/3	d_R^{c2}
$\frac{1}{2}\times$	+	+	−		$\frac{1}{2}\times$			d_R^{c3}
	+	−	−					$\tilde{u}_L^{\bar{c}1}$
0	−	+	−	−1/6	−1/2	−2/3	−2/3	$\tilde{u}_L^{\bar{c}2}$
	−	−	+					$\tilde{u}_L^{\bar{c}3}$
	−	−	−	−1/2		−1	−1	l_R^-

Table 12.2. Eight cases of inversions in the small T-triangle at $\zeta = 3/\sqrt{3}$ with *original* (unchanged) D-triangles at $\zeta = 2/\sqrt{3}$ and $4/\sqrt{3}$, associated with weak-uncharged "down" fermions

The original unchanged state with $Q = 0$ is the vacuum state, so it takes place of the left-handed anti-neutrino, that, according to experiments, does not exist. In

[5] In the (ξ, ζ, υ) reference frame they are $q(\sqrt{2}, \sqrt{3}, 0)$, $q(-\frac{1}{\sqrt{2}}, \sqrt{3}, -\frac{3}{\sqrt{6}})$, $q(-\frac{1}{\sqrt{2}}, \sqrt{3}, \frac{3}{\sqrt{6}})$).

[6] We consider anti-"up" fermions as "down" ones, and vice versa. The "up" particles as well as "up" (anti-"down") anti-particles have the electric charge greater by 1 then the charge of corresponding "down" particles or anti-particles.

$T_3 := q_{(<3)}$	q_3^{210}	q_3^{102}	q_3^{021}	Σq_3	$q_{(>3)}$	$\frac{Y_W}{2} := q_{(\geq 3)}$	Q	symbol
	+	+	+	+1/2		+1/2	0	$\tilde{\nu}_R$
	−	+	+					$d_L^{c_1}$
	+	−	+	+1/6		+1/6	−1/3	$d_L^{c_2}$
$\frac{1}{2}\times$	+	+	−		$\frac{1}{2}\times$			$d_L^{c_3}$
	+	−	−					$\tilde{u}_R^{\tilde{c}_1}$
−1/2	−	+	−	−1/6	0	−1/6	−2/3	$\tilde{u}_R^{\tilde{c}_2}$
	−	−	+					$\tilde{u}_R^{\tilde{c}_3}$
	−	−	−	−1/2		−1/2	−1	l_L^-

Table 12.3. Eight cases of inversions in the small T-triangle at $\zeta = 3/\sqrt{3}$ with *exchanged* D-triangles at $\zeta = 2/\sqrt{3}$ and $4/\sqrt{3}$ associated with weak-charged "down" fermions

this model, the absence of left-handed anti-neutrino is explained by no differences between it and the vacuum state.

Also consider the same cases but combined with *exchanged* D-triangles at $\zeta = 2/\sqrt{3}$ and $4/\sqrt{3}$ (Table 12.3).

12.4.8 Up fermions as Inversions in small T-triangle

Considering the same cases but for the small T-triangle at $\zeta = 9/\sqrt{3}$, we found out that they can be as well associated with "up" fermions. It is so because the shift for half-unit (**S**) from $\zeta = 3/\sqrt{3}$ to $9/\sqrt{3}$ is equal to the **CP** operation. So this triangle and its environment have the reversed handedness and opposite-charged in respect to those considered before.The total charge Q is greater by 1 comparing to the corresponding "down" cases (Table 12.4).

Again, the original vacuum state corresponds to the non-existing particle, that is the right-handed neutrino.

12.5 Polyhedral approximation

Considering the Polyhedral approximation of the dual-charged Weaire-Phelan structure (section 12.3), one can see that walls between cells consist of flat polygonal faces. It is obvious that there are two kinds of walls, since a face can separate either *equal*-charged or *opposite*-charged cells.

Supposing the wall possesses a surface energy E that it is proportional to the face surface area S, and there is a fixed difference in surface density $\Delta\rho$ between both wall kinds, one could estimate the particle mass by the rest energy ΔE associated with a particular defect configuration:

$$m = \Delta E = \Delta\rho \Delta S. \tag{12.18}$$

$T_3 := q_{(<9)}$	$q_9^{4\,2\,3}$	$q_9^{3\,4\,2}$	$q_9^{2\,3\,4}$	Σq_9	$q_{(>9)}$	$Y_W/2 := q_{(\geq 9)}$	Q	
	+	+	+	●●● +1/2		+1	+1	l_L^+
	−	+	+	○●●				u_R^{c1}
	+	−	+	●○● +1/6		+2/3	+2/3	u_R^{c2}
$\frac{1}{2}\times$ ◎●◎	+	+	−	●●○	$\frac{1}{2}\times$ ●●◉			u_R^{c3}
	+	−	−	●○○				$\tilde{d}_L^{\bar{c}1}$
0	−	+	−	○●○ −1/6	+1/2	+1/3	+1/3	$\tilde{d}_L^{\bar{c}2}$
	−	−	+	○○●				$\tilde{d}_L^{\bar{c}3}$
	−	−	−	○○○ −1/2		0	0	$\boxed{\nu_R}$
	+	+	+	●●● +1/2		+1/2	+1	l_R^+
	−	+	+	○●●				u_L^{c1}
	+	−	+	●○● +1/6		+1/6	+2/3	u_L^{c2}
$\frac{1}{2}\times$ ◉●●	+	+	−	●●○	$\frac{1}{2}\times$ ◎●◎			u_L^{c3}
	+	−	−	●○○				$\tilde{d}_R^{\bar{c}1}$
+1/2	−	+	−	○●○ −1/6	0	−1/6	+1/3	$\tilde{d}_R^{\bar{c}2}$
	−	−	+	○○●				$\tilde{d}_R^{\bar{c}3}$
	−	−	−	○○○ −1/2		−1/2	0	ν_L

Table 12.4. Eight cases of inversions in the small T-triangle at $\zeta = 9/\sqrt{3}$, repeated twice with original and exchanged D-triangles at $\zeta = 8/\sqrt{3}$ and $10/\sqrt{3}$, associated with "up" fermions

Since D cell has 6 equal-charged and also 6 opposite-charged neighbors, the inversion does not affect the area ($\Delta S = 0$) and

$$\Delta E_D = 0. \tag{12.19}$$

In contrast, among 14 neighbors of T cell six ones are equal-charged but there are eight opposite-charged ones. Both opposite-charged neighbors that become equal-charged ones in an inversion, are separated with the hexagonal faces with area S_6. So

$$\Delta E_T = 2\Delta\rho S_6. \tag{12.20}$$

Assuming the energy density for wall between equal-charged cells is greater than for opposite-charged ones, $\Delta\rho > 0$ and $\Delta E > 0$.

In case of inversions of *two* neighboring cells, there is an additional effect caused by their common face.

In case two neighbor cells exchange their charge (thus, they are D and T touching each other with large pentagonal face S_{5L} or two T touching each other

with small pentagonal face S_{5s} or hexagonal one S_6) the common face remains separating opposite-charged cells, instead of being turned into separating equal-charged cells, so energy effect is negative:

$$\begin{aligned} \Delta E_{D \leftrightarrows T} &= -2\Delta\rho S_{5L}, \\ \Delta E_{T \leftrightarrows T_5} &= -2\Delta\rho S_{5s}, \\ \Delta E_{T \leftrightarrows T_6} &= -2\Delta\rho S_6. \end{aligned} \tag{12.21}$$

In case of two neighbor cells inverting in the same direction, the additional effect of the common face is opposite, i.e. positive:

$$\begin{aligned} \Delta E_{D \rightrightarrows T} &= 2\Delta\rho S_{5L}, \\ \Delta E_{T \rightrightarrows T_5} &= 2\Delta\rho S_{5s}, \\ \Delta E_{T \rightrightarrows T_6} &= 2\Delta\rho S_6. \end{aligned} \tag{12.22}$$

Note that numerical values of the faces' areas (in units of λ^2) are such that S_{5L} is *almost* equal to the arithmetic mean of S_6 and S_{5s}:

$$\begin{aligned} S_{5L} &\approx 1.77477, \\ S_{5s} &\approx 1.15338, \\ S_6 &\approx 2.41260, \text{ so} \\ S_6 + S_{5s} - 2S_{5L} &\approx 0.0164. \end{aligned} \tag{12.23}$$

Now we can build the simple hierarchical seesaw model of mass based on addition and subtraction of energy effects.

- Since D exchanges have $\Delta E = 0$, massless particles like photon and neutrino must be associated with D-only exchanges.
- Following our 8-bit model [7], associate W^+ boson with five defects combination shown on Fig. 12.9W. Note that it is colorless and has correct electric charge $Q = +1$. The affected area of these defects is

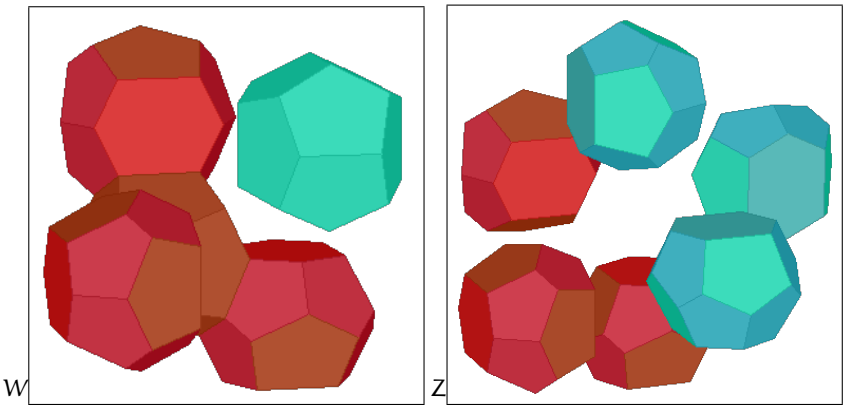

Fig. 12.9. Models of W^+ and Z^0 bosons in polyhedral approximation

$$\Delta S_W = 6\,(S_6 + S_{5L}) = 25.12422. \tag{12.24}$$

Using experimental value of $m_W = 80.385 GeV$ we get

$$\Delta\rho = \frac{m_W}{\Delta S_W} \approx 3.1995\ GeV/\lambda^2. \tag{12.25}$$

- Following the same way, we associate Z^0 boson with neutral six T defect configuration shown on Fig. 12.9Z. Using the same $\Delta\rho$ value, we get

$$m_Z = 12\Delta\rho S_6 \approx 92.629\ GeV. \tag{12.26}$$

- The Higgs boson having, accordingly to 8-bit model, the defects structure similar to Z boson but with one additional D defect pair (Fig. 12.9H), must have one of D cells isolated the same way as W has, to get the appropriate mass:

$$m_H = \Delta\rho(12S_6 + 6S_{5L}) \approx 126.699\ GeV. \tag{12.27}$$

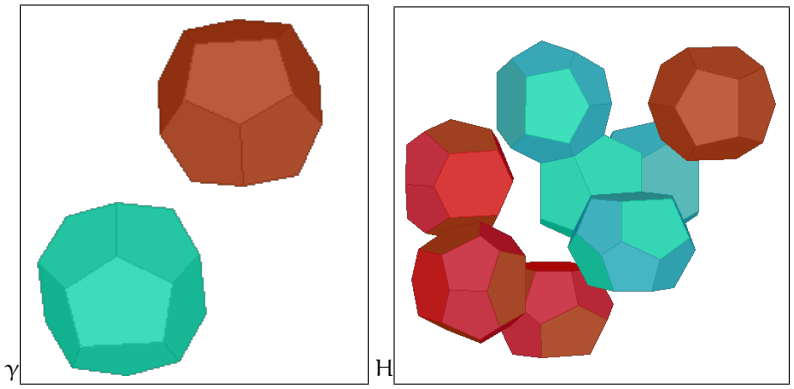

Fig. 12.10. Models of γ photon and H^0 bosons in polyhedral approximation

- For charged lepton we suppose the structure of small-T-triangle inversion combined with eight inversions of D cells providing the compensation (Fig.12.11).This mechanism does not follow the pattern used in 8-bit model for fermion families representation[7], but it offers effective mass reduction below GeV scale.

$$m_l = \Delta\rho(6S_6 - 12S_{5s} + 6S_{5L}) \approx 0.315\ GeV. \tag{12.28}$$

- The zero-charged compensating "frame" consisting from D cells could be associated with massless neutrino (Fig.12.11ν).
- Although the exchange between two or more stacked T cells has the positive energetic effect, its magnitude does not depend on the stack length, and originates just from the non-compensated ends of the stack that has the color charge due to their asymmetry. So it can be associated with the gluon thread terminated with quarks.

[7] the latter involves additional T-D exchange.

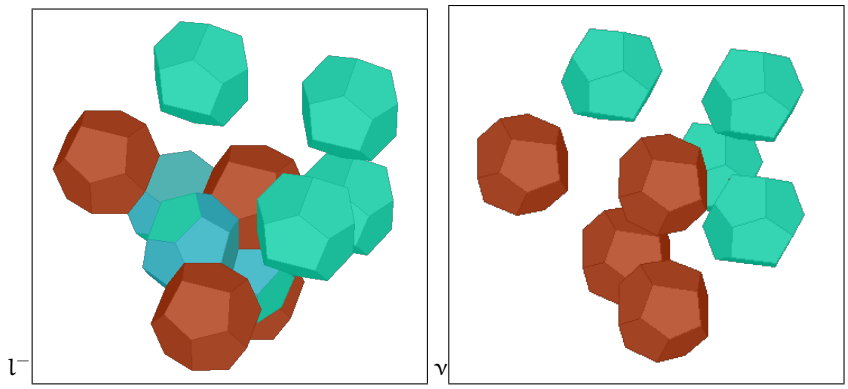

Fig. 12.11. Models of charged lepton with compensated mass, and massless neutrino in polyhedral approximation

12.6 Analytical approximation of charge distribution

In addition to the Polyhedral and Cell-Center approximations we consider an approximation of the structure by the triple-periodical analytical function of electrical charge density distribution.

The electrical charge of the cell concentrated at its center (x_0, y_0, z_0) can be expressed analytically using the δ-function:

$$q = \frac{e}{6} \int\limits_{\mathbb{R}^3} \delta(x - x_0, y - y_0, z - z_0)\, dx\, dy\, dz \tag{12.29}$$

The delta function can be considered as the spherically-symmetrical Gaussian distribution with zero deviation:

$$\delta(x, y, z) = \lim_{\sigma \to 0} \delta(x, y, z, \sigma); \tag{12.30}$$

$$\delta(x, y, z, \sigma) = \frac{1}{(\sigma\sqrt{2\pi})^3} e^{-\frac{x^2+y^2+z^2}{2\sigma^2}} \tag{12.31}$$

As we have shown in section 12.4.6, the model explaining the weak isospin $T_3 = 0$ for right-handed fermions and $T_3 = \pm 1/2$ for left-handed ones by the charge exchange between D-triangles at $\zeta = 2/\sqrt{3}$ and $4/\sqrt{3}$, requires one quarter of the charge of each D cell to reside behind the section plane located at the distance of $1/\sqrt{3}$ from the cell center:

$$\int\limits_{x=-\infty}^{-1/\sqrt{3}} \int\limits_{y=-\infty}^{+\infty} \int\limits_{z=-\infty}^{+\infty} \rho(x, y, z)\, dx\, dy\, dz = \frac{1}{4} \tag{12.32}$$

Assuming charge density $\rho(x, y, z)$ to be the Gaussian distribution (12.31), and solving the equation

$$\frac{1}{(\sigma\sqrt{2\pi})^3} \int\limits_{x=-\infty}^{-1/\sqrt{3}} \int\limits_{y=-\infty}^{+\infty} \int\limits_{z=-\infty}^{+\infty} e^{-\frac{x^2+y^2+z^2}{2\sigma^2}}\, dx\, dy\, dz = \frac{1}{4} \tag{12.33}$$

numerically, we found $\sigma \approx 0.87377$.

Soliton model To construct the charge distribution in the analytical form, we can use, instead of each cell, some spherical-symmetrical function, which decreases quite rapidly on distance from its center, i.e. soliton.

We consider the soliton function as normalized error function

$$\rho_i = \pm \frac{e}{6\sigma\sqrt{2\pi}} \exp\left[-\frac{(x-x_i)^2 + (y-y_i)^2 + (z-z_i)^2}{2\sigma^2}\right], \tag{12.34}$$

representing positive or negative charged cell with the center at (x_i, y_i, z_i). The charge density in the particular point is calculated as a sum of contributions of all the cells in the model:

$$\rho = \sum_i \rho_i \tag{12.35}$$

One can manage the position and charge of each individual cell, so this model should be flexible. On another hand, it requires extensive computation to calculate each point.

Triple-periodic trigonometric function Since the most interesting application of this model is to represent the only one or several defects being surrounded by the "pure" vacuum, we looked for the periodic function that has the same symmetry as the dual-charged Weaire-Phelan structure considered above. It is intended to represent the pure vacuum avoiding calculating of plenty periodically allocated solitons.

At first, we consider the real function that has zero surface close to the Schwartz P minimal surface [15].

$$\rho_0 = \cos x + \cos y + \cos z, \tag{12.36}$$

or, equivalently,

$$\rho_0 = \sum_i \cos x_i. \tag{12.37}$$

$$\rho_0 = \cos\frac{x\pi}{2\lambda} + \cos\frac{y\pi}{2\lambda} + \cos\frac{z\pi}{2\lambda}, \tag{12.38}$$

It has minimum in points $(2\pi n_x, 2\pi n_y, 2\pi n_z) = 2\pi(n_x, n_y, n_z)$ and maximum in $\pi(2n_x+1, 2n_y+1, 2n_z+1)$ since

$$\frac{\partial \rho_0}{\partial x_i} = -\sin x_i = 0 \Rightarrow x_i = \pi n_i, \tag{12.39}$$

and

$$\frac{\partial^2 \rho_0}{\partial x_i^2} = -\cos x_i. \tag{12.40}$$

The last equation also means that

$$\Delta\rho_0 = -\rho_0, \tag{12.41}$$

so ρ_0 is eigenfunction of the Laplasian, with eigenvalue -1.

The translation unit with $n_x = n_y = n_z = 0$ is a cube with $x_i \in [-\pi; \pi]$.

So, ρ_0 has one minimum in $(0, 0, 0)$ and one maximum in $\frac{\pi}{4}(2, 2, 2)$.

As the second step, we consider the surface $\rho_0 = 0$. Its saddle points are the same with the T cell center points. So we can add the function with extremals at these points, namely at centers of D cells:

$$\rho_{xz} = \frac{1}{4} \sin y(1 - \cos x)(1 + \cos z) \tag{12.42}$$

$$\rho_{yx} = \frac{1}{4} \sin z(1 - \cos y)(1 + \cos x) \tag{12.43}$$

$$\rho_{zy} = \frac{1}{4} \sin y(1 - \cos z)(1 + \cos y) \tag{12.44}$$

$$\rho_{xy} = \frac{1}{4} \sin z(1 - \cos x)(1 + \cos y) \tag{12.45}$$

$$\rho_{yz} = \frac{1}{4} \sin y(1 - \cos y)(1 + \cos z) \tag{12.46}$$

$$\rho_{zx} = \frac{1}{4} \sin y(1 - \cos z)(1 + \cos x) \tag{12.47}$$

$$\rho_R = \rho_{xy} + \rho_{yz} + \rho_{zx} \tag{12.48}$$

$$\rho_L = \rho_{yx} + \rho_{zy} + \rho_{xz} \tag{12.49}$$

We construct right and left vacuum electric charge density as

$$\rho_{0R} = \rho_0 + \rho_R \tag{12.50}$$

$$\rho_{0L} = \rho_0 + \rho_L. \tag{12.51}$$

Note that ρ_{xz} (12.42) and other ρ_{ij} can be rewritten in the following way:

$$\rho_{xz} = \frac{1}{4} \left(\sin y + \sin y \cos z - \sin y \cos x - \sin y \cos x \cos z \right), \tag{12.52}$$

so ρ_R and ρ_L can be represented as sums of four functions listed below, which accumulate summands of four particular types, that occur in (12.42).

Introducing "Schwartz P"- like distribution

$$P_\theta = \cos(x - \theta) + \cos(y - \theta) + \cos(z - \theta), \tag{12.53}$$

right and left gyroid-like distributions

$$G_R = \cos x \sin y + \cos y \sin z + \cos z \sin x, \tag{12.54}$$

$$G_L = \cos x \sin z + \cos y \sin x + \cos z \sin y, \tag{12.55}$$

and "layers-with-holes" distribution

$$H = \cos x \sin y \cos z + \cos y \sin z \cos x + \cos z \sin x \cos y, \tag{12.56}$$

we can express ρ_R through them:

$$\rho_{0R} = \frac{1}{4}\left[P_{\pi/2} + G_L - G_R - H\right] - \frac{1}{3}P_0. \tag{12.57}$$

Since G and H are also eigenfunctions of the Laplasian Δ:

$$\Delta G = -2G; \Delta H = -3H, \tag{12.58}$$

one can find the scalar electric potential:

$$\operatorname{div}\operatorname{grad}\varphi_{0R} = \Delta\varphi_{0R} = 4\pi\rho_{0R}, \tag{12.59}$$

$$\varphi_{0R} = +\frac{1}{12\pi}P_0 - \frac{1}{16\pi}\left[P_{\pi/2} + \frac{1}{2}G_L - \frac{1}{2}G_R - \frac{1}{3}H\right]. \tag{12.60}$$

Combining triple-periodical trigonometric equation for the vacuum state with doubled opposite-charged soliton located in particular cell centers one can obtain a model representing one or more particles surrounded by the vacuum.

12.7 Discussion

12.7.1 Two-dimension model

Consider the surface of zero potential (12.60):

$$\varphi_{0R} = +\frac{1}{12\pi}P_0 - \frac{1}{16\pi}\left[P_{\pi/2} + \frac{1}{2}G_L - \frac{1}{2}G_R - \frac{1}{3}H\right] = 0. \tag{12.61}$$

It defines the manifold with the mostly negative Gaussian curvature that can be studied using two-dimensional Einstein GRT equation.

The three-dimensional space, discrete with the grid size $l \approx 4 \cdot 10^{-21}$m, appears in this model as a result of the foam-like structure of this two-dimensional manifold. So the continuous three-dimensional space can be considered just as an asymptotic on distances lager than the grid size. As a consequence of this approach, the three-dimensional gravity should not be considered in its usual form on distances comparable to or less than the grid size.

12.7.2 Liquid-Liquid Phase Transition model

We suppose that the structures close to one considered above can emerge in systems possessing 2-order phase transition near the critical point, for instance, in liquid-liquid mixtures like $H_2O - -C_6H_5OH$.

12.7.3 Other topics

There are some topics that we'd like to mention here as directions in which the research can be continued.

Firstly, it is the dynamics. Each defect in the vacuum structure is supposed to be able to change its localization. It can be considered from several viewpoints listed above and also using other approaches, for instance, the cellular automata.

Secondly, the interactions and the virtual particles. Our approach can be also applied to bosons. Some 'bosonic' exchanges seem to have no influence on the two-dimensional manifold topology, so there is no sharp difference between particles (defects) and classical fields (distortions).

Thirdly, there can be another structures with the properties allowing to use them as a model of vacuum and particles. We have found and tested just one.

12.8 Conclusion

We presented here our approach to the particle and vacuum modeling, based on the assumption that on scale $\approx 10^{-19}$ cm there are areas with non-zero electrical charge density and they are self-assembled in the structure close to the Weaire-Phelan tessellation. This structure possesses **CPS** symmetry and allows the existence of anti-structure defects in it, that can be corresponded to known fundamental particles (at least, for one fermion family), reproducing their known properties.

References

1. N.S. Mankoč Borštnik, "Can spin-charge-family theory explain baryon number non conservation?", *Phys. Rev.* **D 91** (2015) 6, 065004, [arXiv:1502.06786v1]
2. N. Mankoč Borštnik, "Spinor and vector representations in four dimensional Grassmann space", *J. of Math. Phys.* **34** (1993), 3731-3745.
3. Ya. B. Zeldovich, I. Yu. Kobzarev, and L. B. Okun': Cosmological consequences of a spontaneous breakdown of a discrete symmetry: Zh. Eksp. Teor. Fiz. 67, 3-11 (July 1974) [Sov. Phys. JETP 40, 1 (1974)].
4. Nordström, Gunnar (1914). "Über die Möglichkeit, das elektromagnetische Feld und das Gravitationsfeld zu vereinigen". Physikalische Zeitschrift. 15: 504–506. OCLC 1762351.
5. Kaluza, Theodor (1921). "Zum Unitätsproblem in der Physik". Sitzungsber. Preuss. Akad. Wiss. Berlin. (Math. Phys.): 966–972. https://archive.org/details/sitzungsberichte1921preussi
6. Klein, Oskar (1926). "Quantentheorie und fünfdimensionale Relativitätstheorie". Zeitschrift für Physik A. 37 (12): 895–906. Bibcode:1926ZPhy...37..895K. doi:10.1007/BF01397481.
7. E.G. Dmitrieff: Experience in modeling properties of fundamental particles using binary codes, in: N.S. Mankoč Borštnik, H.B.F. Nielsen, D. Lukman: Proceedings to the 19th Workshop 'What Comes Beyond the Standard Models', Bled, 11. - 19. July 2016.
8. N.S. Mankoč Borštnik, "The explanation for the origin of the higgs scalar and for the Yukawa couplings by the *spin-charge-family* theory", *J. of Mod. Physics* **6** (2015) 2244-2274, [arXiv:1409.4981]
9. N.S. Mankoč Borštnik, "Spin-charge-family theory is offering next step in understanding elementary particles and fields and correspondingly universe", 10^{th} IARD conference,Ljubljana 2016, J. Phys.: Conf. Ser. 845 (2017) 012017 and references therein [arXiv:1607.01618v2]

10. Kittel, Charles: Introduction to Solid State Physics (8th ed.). John Wiley & Sons, Inc. (2004).
11. E.G. Dmitrieff: The Hypothesis of Unity of the Higgs Field With the Coulomb Field, in: N.S. Mankoč Borštnik, H.B.F. Nielsen, D. Lukman: Proceedings to the 19th Workshop 'What Comes Beyond the Standard Models', Bled, 11. - 19. July 2016.
12. D.Weaire, R.Phelan: A counter-example to Kelvin's conjecture on minimal surfaces, Phil. Mag. Lett., (1994) 69: 107–110, doi:10.1080/09500839408241577
13. Ruggero Gabbrielli, Aaron J. Meagher, Denis Weaire, Kenneth A. Brakke & Stefan Hutzler (2012) An experimental realization of the Weaire–Phelan structure in monodisperse liquid foam, Philosophical Magazine Letters, 92:1, 1-6, DOI: 10.1080/09500839.2011.645898
14. Lord Kelvin (Sir William Thomson) (1887), "On the Division of Space with Minimum Partitional Area" (PDF), Philosophical Magazine, 24 (151): 503, doi:10.1080/14786448708628135
15. Alan H. Schoen: Infinite periodic minimal surfaces without self-intersections, NASA Technical Note TN D-5541 (1970)